ELSEVIER

15 June 1997

Optics Communications 139 (1997) 157–164

OPTICS COMMUNICATIONS

Full length article

Wigner function for a generalized model of a parametric oscillator: phase-space tristability, competition and nonclassical effects

K.V. Kheruntsyan [a], D.S. Krähmer [b], G.Yu. Kryuchkyan [a,b], K.G. Petrossian [a]

[a] *Institute for Physical Research, National Academy of Sciences of Armenia, Ashtarak-2 378410, Armenia*
[b] *Abteilung für Quantenphysik, Universitat Ulm, D-89069 Ulm, Germany*

Received 24 May 1996; revised 30 October 1996; accepted 27 November 1996

Abstract

We present an exact quantum treatment of the generalized model of a degenerate parametric oscillator, in which we allow for self-phase modulation of the signal mode. Using the steady-state solution of the Fokker-Planck equation in the complex P-representation we obtain an exact analytical result for the Wigner quasiprobability distribution function. The obtained Wigner function allows us to give an explicit phase-space description of the nonlinear system under consideration, including the critical transition behavior in the monostable and bistable (with respect to the signal mode intensity versus the pump field intensity) operation regimes and in the threshold region. The competitive effects influenced by the self-phase modulation and the phase-space tristability are analyzed. Nonclassical effects of quadrature squeezing and quantum superposition are discussed as well.

1. Introduction

Recently the Wigner function $W(\alpha)$, which is a joint quasiprobability distribution for the position $x = \mathrm{Re}\,\alpha$ and the momentum $y = \mathrm{Im}\,\alpha$ of a quantum system, became a subject of increasing interest in quantum optics. It has a number of advantages when compared with other quasiprobability distributions. In particular, it is never singular and describes best nonclassical states of light in phase space [1–3]. Moreover, the Wigner function can be tomographically reconstructed from experimental data by measurements of a set of probability distributions of the light quadrature-phase amplitudes [4–6]. Nevertheless, very little work has been devoted to the calculation of the Wigner function for realistic quantum optical models including particular nonlinear interactions and dissipation.

In this paper we present an exact analytical result for the steady-state Wigner function describing the model of a degenerate parametric oscillator (PO) (in the sub-harmonic generation configuration), which is well known as one of the most fundamental devices in quantum optics. In our analysis we include the pump depletion and arbitrary cavity detunings which lead to a rich variety of phase transitions and dynamical behavior. They have been studied at the semiclassical level in a number of works (see, e.g., Refs. [7–9]). In addition, our model combines the effect of self-phase modulation (SPM) of the signal mode due to the $\chi^{(3)}$-susceptibility of the nonlinear medium.

The quantum dynamics and nonclassical properties of the PO have been extensively studied in the literature (see, e.g., Refs. [7,8,10,11]). The studies show, in particular, that the main interesting features of PO can be described within the ranges of linear approximation of light quantum fluctuations. However, to obtain the most complete and precise predictions, applicable in all possible regimes of operation including the threshold region, one needs to deal with the exact nonlinear treatment of quantum fluctuations. In this field of research the most detailed analysis of the PO has been carried out [12,13] with the use of the solution of the Fokker-Planck equation in the positive

PII S0030-4018(96)00753-5

P-representation. It should be pointed out, however, that the results obtained on the basis of the positive P-representation are related to the case of zero cavity detunings and hence they do not describe the PO in the regime, when the signal mode intensity is bistable.

The general solution of the Fokker-Planck equation in the complex P-representation, describing the PO in the unified sub/second-harmonic generation configuration has been obtained for the first time in Ref. [7b]. As to the Wigner function for PO, its approximate calculation has been presented, in particular, in Ref. [13] on the basis of the corresponding truncated Fokker-Planck equation and for the case of zero cavity detunings. Calculation and analysis of the Wigner function for nondetuned PO have been given also in Ref. [14] on the basis of the positive P-representation. We note also that an exact quantum treatment of the process of SPM of a cavity mode which is parametrically driven via the process of subharmonic generation, has been presented in Ref. [15].

In the present paper we develop an exact quantum theory for the generalized model of PO, which combines the processes of sub-harmonic generation and the SPM of the signal mode. Possible nonzero cavity detunings are taken into account. We find the steady-state solution of the Fokker-Planck equation in the complex P-representation. The Wigner function is then calculated analytically with use of its relation with the complex P-representation. The final result for the Wigner function has a rather simple form. We use this result to study the behavior of our nonlinear system in the phase space. In particular, we analyze the critical-transition phenomena in the mono- and bi-stable operation regimes and discuss the peculiarities of the quadrature squeezing effect. The oscillatory behavior of the Wigner function, which is known as an indicative of quantum superposition and interference, is discussed as well.

2. Model Hamiltonian and Fokker-Planck equation

We consider a doubly resonant cavity which supports two resonant modes – the signal and the pump modes at frequencies ω_s and ω_p ($\omega_p \cong 2\omega_s$), respectively. The pump mode is driven by an external classical driving field at frequency $\omega_0 \cong \omega_p$, while the signal mode is excited, via a nonlinear medium with $\chi^{(2)}$-nonlinearity, through the parametric process of frequency down-conversion. In addition, the signal mode is allowed to undergo the process of SPM (Kerr interaction) via the $\chi^{(3)}$-nonlinearity. The signal and the pump modes suffer losses due to cavity losses. We adopt the following model Hamiltonian:

$$H = H_0 + H_{\rm int} + H_{\rm loss}, \tag{1}$$

where

$$H_0 = \hbar\omega_s a^+ a + \hbar\omega_p b^+ b, \tag{2}$$

$$H_{\rm int} = \mathrm{i}\frac{\hbar k}{2}(a^{+2}b - b^+ a^2) + \mathrm{i}\hbar(E\,\mathrm{e}^{-\mathrm{i}\omega_0 t}b^+ - E^*\,\mathrm{e}^{\mathrm{i}\omega_0 t}b) + \frac{\hbar\chi}{4}a^{+2}a^2, \tag{3}$$

$$H_{\rm loss} = \Gamma_s^+ a + a^+\Gamma_s + \Gamma_p^+ b + b^+\Gamma_p. \tag{4}$$

Here a (a^+) and b (b^+) are annihilation (creation) operators for the signal and the pump modes, k and χ are the coupling constants proportional to the $\chi^{(2)}$- and $\chi^{(3)}$-susceptibilities, and E is the driving field amplitude. The three terms in $H_{\rm int}$ describe the parametric interaction, the coherent driving of the pump mode, and the SPM of the signal mode, respectively. $H_{\rm loss}$ is responsible for linear losses of the signal and the pump modes due to coupling with reservoirs, with Γ_s, Γ_s^+ and Γ_p, Γ_p^+ being the usual reservoir operators giving rise to the cavity damping rates γ_s and γ_p.

We follow the standard procedures (see, e.g., Refs. [1,2]) to eliminate the reservoir operators and to obtain a master equation for the reduced density operator ρ of the signal and the pump modes. The master equation is then transformed into a Fokker-Planck equation in the complex P-representation [2]. Assuming at this stage that the pump mode has high cavity losses ($\gamma_p \gg \gamma_s$) and hence may be eliminated adiabatically, one can obtain the following Fokker-Planck equation for the signal mode:

$$\frac{\partial}{\partial t}P(\alpha,\alpha^+) = \left\{-\frac{\partial}{\partial\alpha}\left[-\bar{\gamma}\alpha + (\mu - \nu\alpha^2)\alpha^+\right] - \frac{\partial}{\partial\alpha^+}\left[-\bar{\gamma}^*\alpha^+ + (\mu^* - \nu^*\alpha^{+2})\alpha\right] + \frac{1}{2}\frac{\partial^2}{\partial\alpha^2}\left[\mu - \nu\alpha^2\right] + \frac{1}{2}\frac{\partial^2}{\partial\alpha^{+2}}\left[\mu^* - \nu^*\alpha^{+2}\right]\right\}P(\alpha,\alpha^+). \tag{5}$$

Here α and α^+ are independent complex c-number variables corresponding to the operators a and a^+, respectively, and we have introduced the following notations:

$$\mu \equiv \frac{kE}{\bar{\gamma}_p}, \quad \nu \equiv \frac{k^2}{2\bar{\gamma}_p} + \mathrm{i}\frac{\chi}{2} = \frac{k^2\gamma_p}{2|\bar{\gamma}_p|^2} + \mathrm{i}\left(\frac{k^2\Delta_p}{2|\bar{\gamma}_p|^2} + \frac{\chi}{2}\right), \tag{6}$$

$$\bar{\gamma} \equiv \gamma_s - \mathrm{i}\Delta_s, \quad \bar{\gamma}_p \equiv \gamma_p - \mathrm{i}\Delta_p, \tag{7}$$

where $\Delta_s = \omega_0/2 - \omega_s$ and $\Delta_p = \omega_0 - \omega_p$ are the cavity detunings for the signal and the pump modes, μ is the parametric coupling coefficient, and ν is the resulting nonlinearity coefficient containing the contributions from the back action of the pump mode on the signal and from the process of SPM. We see that the contribution from SPM changes the imaginary part of ν as compared to its value in the case of pure PO.

3. Steady-state solution of the Fokker-Planck equation and the Wigner function

To analyze the behavior of our nonlinear system within the ranges of exact nonlinear treatment of quantum fluctuations we use the solution of the Fokker-Planck equation (5) in the steady-state regime. The steady-state solution can be found using the method of potential equations [1,2]. This yields

$$P_s(\alpha,\alpha^+) = N\left(\frac{\mu}{\nu} - \alpha^2\right)^{\lambda-1}\left(\frac{\mu^*}{\nu^*} - \alpha^{+2}\right)^{\lambda^*-1} \times \exp(2\alpha\alpha^+), \tag{8}$$

where

$$\lambda \equiv \frac{\bar{\gamma}}{\nu} = \frac{\gamma_s \operatorname{Re}\nu - \Delta_s \operatorname{Im}\nu}{|\nu|^2} - i\frac{\gamma_s \operatorname{Im}\nu + \Delta_s \operatorname{Re}\nu}{|\nu|^2}, \tag{9}$$

and N is the normalization constant.

We note that the complex quasiprobability P-function (8) coincides formally with that of the pure PO [7b]. The difference consists in the definition of the parameter ν: if we neglect the contribution from the SPM and take $\chi = 0$, we obtain the known result for pure PO. On the other hand, the form (8) of the P-function coincides with that of a more simplified version of our present nonlinear model. This simplified model has been studied in Ref. [15] and has been called parametrically driven anharmonic oscillator (PDAO). It is related to complete neglecting the pump depletion and describes the process of SPM of the signal mode which is driven via a direct parametric pumping by a classical field. The results for the PDAO model can be obtained from the present ones by setting $\mu = kE/\gamma_p$ and $\nu = i\chi/2$.

The steady-state solution (8) is sufficient to calculate normally ordered operator moments and to study various quantum statistical characteristics of the signal mode in terms of the mean values of the quantities of interest. For the simplified PDAO model particular results have been presented in Ref. [15]. However, in the present paper we are interested in the phase-space description of our generalized model. We shall display and analyze the phase-space properties in terms of the Wigner function:

$$W(\alpha) = \frac{1}{\pi^2}\int d^2\gamma \operatorname{Tr}\left(\rho e^{\gamma a^+ - \gamma^* a}\right) e^{\gamma^*\alpha - \gamma\alpha^*}. \tag{10}$$

We calculate the Wigner function using its relation with the complex P-representation of the density matrix ρ. Writing down the definition of ρ in terms of the complex P-function

$$\rho = \iint_{CC'} d\beta\, d\beta^+ \frac{|\beta\rangle\langle\beta^{+*}|}{\langle\beta|\beta^{+*}\rangle} P(\beta,\beta^+), \tag{11}$$

where C and C' are appropriate integration paths for β and β^+ variables, we then transform in Eq. (10) to the normal ordering of operators and, using the correspondence between the normally ordered operator averages and the c-number averages in P-representation, we arrive at the following relation:

$$W(\alpha) = \frac{2}{\pi} e^{-2|\alpha|^2}\int_C\int_{C'} d\beta\, d\beta^+ P(\beta,\beta^+) \times e^{2\alpha^*\beta + 2\alpha\beta^+ - 2\beta\beta^+}. \tag{12}$$

Substituting the steady-state complex P-function (8) into (12) we see that the exponential term $\exp(-2\beta\beta^+)$ in (12) cancels the term $\exp(2\beta\beta^+)$ in $P(\beta,\beta^+)$. This leads directly to a separation of the integral variables, that simplifies the integrations substantially. Noting also that the integrals become identical to those in the definition of the Bessel-function $J_\nu(z)$ [16], with C (C') being an eight-shaped contour encircling the points ± 1 on the complex plane, we obtain the following final result for the steady-state Wigner function:

$$W_s(\alpha) = N_1 e^{-2|\alpha|^2}\frac{|J_{\lambda-1/2}(2\alpha^*\sqrt{r}\, e^{i\vartheta})|^2}{|(\alpha^*)^{\lambda-1/2}|^2}, \tag{13}$$

where N_1 is the corresponding normalization constant, and we have introduced the following notations

$$r = |\mu|/|\nu|, \quad \vartheta = \tfrac{1}{2}(\pi + \phi_\mu - \phi_\nu), \tag{14}$$

with ϕ_μ and ϕ_ν being the phases of the parameters $\mu = |\mu|\exp(i\phi_\mu)$ and $\nu = |\nu|\exp(i\phi_\nu)$.

As is known the Wigner function $W(\alpha)$, being a joint quasiprobability distribution for the position $x = \operatorname{Re}\alpha$ and the momentum $y = \operatorname{Im}\alpha$ of a quantum system, can take negative values for some x and y. The negativeness of the Wigner function is one of the indicatives of nonclassical properties of the state of the system [2,3]. In relation with this, we point out that for our nonlinear system the steady-state Wigner function (13) is always positive. This property is originated from the specific form of our interaction Hamiltonian. It contains only quadratic terms with respect to the signal mode creation and annihilation operators a^+ and a, implying that in our system we deal only with pair transformations of photons of the signal mode.

4. Semiclassical steady states and competition effects

To proceed with further analysis we shall present now the semiclassical steady-state solutions and stability properties of the nonlinear system under consideration. The equation of motion that governs the behavior of the signal mode amplitude in the semiclassical approximation is

$$d\alpha/dt = -\bar{\gamma}\alpha + (\mu - \nu\alpha^2)\alpha^*. \tag{15}$$

Solving this equation for the steady states and carrying out the standard linearized stability analysis one can arrive at the following results. We express them in terms of the parameters λ and r, introduced in Eqs. (9) and (14).

The trivial zero-amplitude solution $\alpha_0 = 0$, which describes the below-threshold regime of oscillation, is stable in the region

$$r < r_{th}, \quad r_{th} = |\lambda|, \tag{16}$$

with r_{th} being the threshold value of the amplitude of the relation μ/ν.

The nonzero above-threshold solutions, expressed in terms of the intensity n_0 (in photon number units) and the phase ϕ_0 of the signal mode ($\alpha_0 = \sqrt{n_0}\ \exp(i\phi_0)$) are determined by the following expressions:

$$n_0 = -\mathrm{Re}\lambda \pm \sqrt{r^2 - (\mathrm{Im}\lambda)^2}, \tag{17}$$

$$\sin(2\phi_0 - \phi_\mu + \phi_\nu) = -\frac{\mathrm{Im}\lambda}{r}. \tag{18}$$

The minus sign in front of the square root in Eq. (17) corresponds to the unstable solution. The solution with plus sign is stable in the following domains

$$r > r_{th}, \quad \text{if } \mathrm{Re}\lambda > 0, \tag{19}$$

$$r > |\mathrm{Im}\lambda|, \quad \text{if } \mathrm{Re}\lambda < 0. \tag{20}$$

We see that the signal intensity n_0 depending on the intensity parameter of the pump field r^2 shows bistable behavior in the case $\mathrm{Re}\lambda < 0$. The bistability domain for r is $|\mathrm{Im}\lambda| < r < r_{th}$. On the other hand, Eqs. (17) and (18) imply that in the above-threshold regime there exist actually two stable steady states, which have equal intensities n_0 but opposite phases ϕ_0 and $\phi_0 + \pi$, i.e. we observe a phase bistability.

The general behavior of the signal mode intensity n_0 depending on the scaled pump intensity parameter r^2 is represented in Fig. 1.

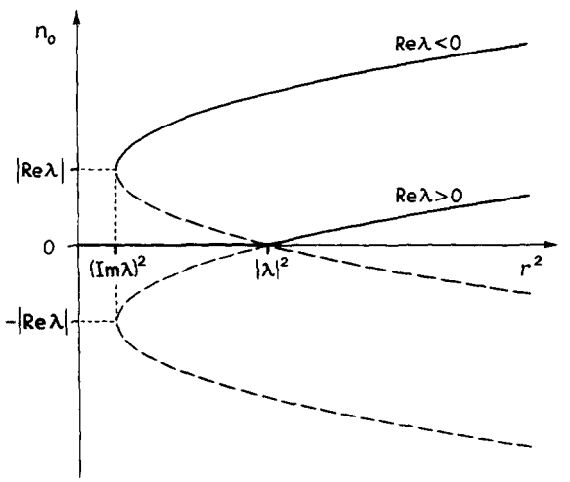

Fig. 1. The semiclassical steady-state intensity of the signal mode n_0 plotted against the intensity parameter r^2 of the pump field for $|\mathrm{Re}\lambda|/|\mathrm{Im}\lambda| = 2$. The dashed parts of the curves are related to the unstable unphysical steady-state solutions.

In terms of the pump intensity $|E|^2$, the oscillation threshold can be rewritten in the following explicit form:

$$|E_{th}|^2 = \frac{(\gamma_s^2 + \Delta_s^2)(\gamma_p^2 + \Delta_p^2)}{k^2}, \tag{21}$$

while the condition of bistability occurrence ($\mathrm{Re}\lambda < 0$) becomes

$$k^2(\Delta_s\Delta_p - \gamma_s\gamma_p) + \chi\Delta_s(\gamma_p^2 + \Delta_p^2) > 0. \tag{22}$$

Considering an application of the above results to the case of pure PO we notice, in particular, that in this case ($\chi = 0$) the bistability condition becomes $\Delta_s\Delta_p > \gamma_s\gamma_p$ [8,9]. As to the case of the simplified PDAO model, in which the pump depletion and hence its back action on the signal is completely neglected ($\nu = i\chi/2$), this condition is simplified to $\Delta_s > 0$ [15].

In the general case, we conclude that the inclusion of SPM into our generalized PO model leads to competition-like effects and gives us an additional possibility to control the behavior of the system. In particular, in the case $\Delta_s\Delta_p > \gamma_s\gamma_p$ and if $\Delta_s > 0$ the SPM can make the bistable behavior of the signal intensity more pronounced. Moreover, it can lead to bistability occurrence even in the case of relatively small detunings $\Delta_s\Delta_p < \gamma_s\gamma_p$, when the pure PO is not bistable. In this case we obtain also another gain, that the absolute threshold (21) becomes smaller. If however $\Delta_s < 0$, the influence of the SPM is towards to the monostable behavior of the signal intensity. The origin of the competitive influence of the SPM becomes clear also from the observation that the imaginary part of the resulting nonlinearity coefficient ν (see Eq. (6)) acquires an additional possibility to be varied due to the contribution of the χ coefficient.

5. Critical transition behavior of the Wigner function and squeezing effects

We turn now to the quantum statistical treatment of the critical transitions in our generalized PO model. We consider the steady-state Wigner function (13) and plot it in Cartesian coordinates $x = \mathrm{Re}\alpha$ and $y = \mathrm{Im}\alpha$ for both monostable and bistable cases of the behavior of the signal mode semiclassical intensity.

As it has been shown in the previous section, the bistable behavior of the steady state intensity n_0 takes place for $\mathrm{Re}\lambda < 0$ and the bistability domain is determined by $|\mathrm{Im}\lambda| < r < r_{th}$. In Fig. 2 we plot the Wigner function for the case $\lambda = -20 - 10i$ and scan the parameter r, which characterizes the scaled amplitude of the pump field. We see that below the bistability domain the Wigner function is single-humped and centered at $x = y = 0$ (see Fig. 2a). This hump corresponds to the below-threshold semiclassical steady state ($n_0 = 0$). With increasing r we enter into the critical transition (bistability) domain and observe the occurrence of two additional side-humps. They

correspond to the above-threshold steady states with equal intensities and opposite phases. Hence, we see explicitly that in this domain the behavior of our nonlinear system is actually tristable (see Fig. 2b). With further increase in r, the central hump disappears, while the side-humps increase and we turn to a manifestly above-threshold oscillation regime when we observe (Fig. 2c) only phase bistability. We note that the critical domain of variation of the parameter r, in which the coexisting three humps acquire commensurable heights and each of them can be clearly visualized on the same plot in a proportional scale, is much narrower ($13 \leq r \leq 14$ for $\lambda = -20 - 10\mathrm{i}$) than the corresponding semiclassical bistability domain ($\mathrm{Im}\,\lambda = 10 < r < r_{th} \cong 22.36$).

To illustrate the competitive effects discussed in the previous section we give now particular specifications of

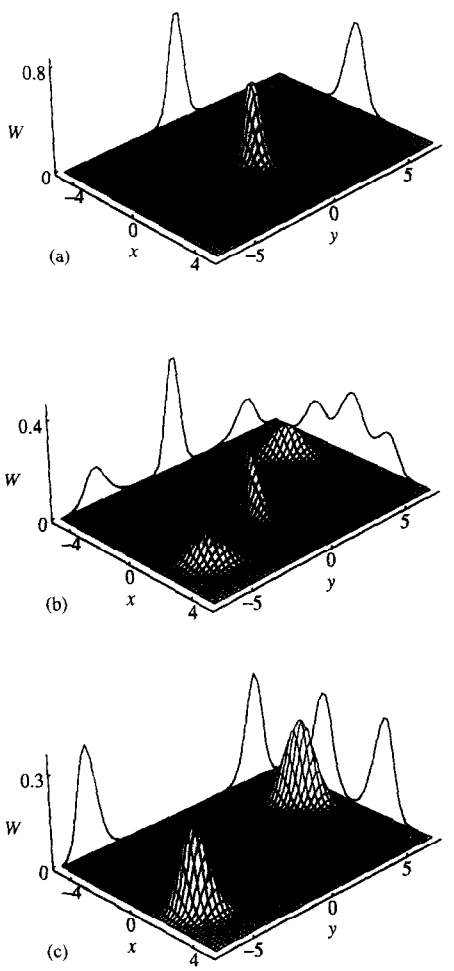

Fig. 2. The steady-state Wigner function $W_s(x,y)$ in the presence of bistability (referred to n_0 versus r^2) for $\lambda = -20 - 10\mathrm{i}$ ($r_{th} \cong 22.36$) and $\theta = \pi$. The parameter r is scanned to demonstrate the critical transition behavior of $W_s(x,y)$ in the bistability domain: (a) $r = 6.25$; (b) $r = 13.32$; (c) $r = 16$. The corresponding marginal distributions $P(x)$ and $P(y)$ are shown in the backgrounds.

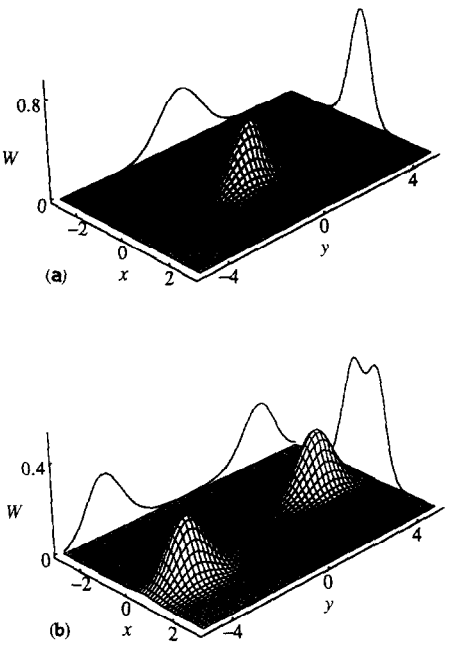

Fig. 3. The steady-state Wigner function and the marginal distributions in the absence of bistability for $\lambda = 20 - 10\mathrm{i}$ ($r_{th} \cong 22.36$) and $\theta = \pi$: (a) $r = 16$; (b) $r = 33$.

the relevant parameters, giving rise to the $\lambda = -20 - 10\mathrm{i}$ value of Fig. 2. For example, this λ value can be realized by considering the following two limiting cases: (i) simplified PDAO model, in which we set $\nu = \mathrm{i}\chi/2$ ($\mathrm{Re}\,\nu = 0$) and choose $\Delta_s/\gamma_s = 2$ and $\chi/2\gamma_s = 0.1$; (ii) pure PO model ($\chi = 0$), in which one may set $\Delta_s/\gamma_s = -3$, $\Delta_p/\gamma_p = -7$ and $\mathrm{Re}\,\nu/\gamma_s = 0.02$.

Fig. 3 shows the Wigner function for the case $\lambda = 20 - 10\mathrm{i}$, when the semiclassical intensity of the signal is monostable. In contrast to the case of Fig. 2, now we just change the sign of $\mathrm{Re}\,\lambda$, retaining $r_{th} \cong 22.36$. We see explicitly the change of the critical transition scenario. In the below-threshold domain the Wigner function is single-humped. However, while transiting the critical threshold point, this hump just splits into two humps which correspond to the above-threshold steady states of equal intensities but opposite phases.

In Fig. 4 we give examples of the Wigner function for pure PO ($\chi = 0$) with $\lambda = 100$ (in this case the semiclassical intensity is monostable, and we choose for simplicity $\Delta_s = \Delta_p = 0$ and $\mathrm{Re}\,\nu/\gamma_s = 0.01$). Similar result for the Wigner function in the case of nondetuned PO has been obtained in Ref. [14] using positive P-representation. It should be pointed out also that the Wigner function for the below-threshold PO, emitting a quadrature squeezed signal, has been tomographically reconstructed in the experiment [6] from a set of measured quadrature-phase amplitude probability distributions. We note that our corresponding result is in qualitative agreement with that of the above experiment.

The squeezing effects can be revealed from our results by considering the quadrature amplitude probability distributions. They are plotted in the backgrounds of Figs. 2–4. The probability distribution $P(x,\phi)$ for any quadrature amplitude operator $X_\phi = [a\exp(-i\phi) + a^+\exp(i\phi)]/2$ can be obtained by integrating the Wigner function over the conjugate quadrature [4]:

$$P(x,\phi) = \int_{-\infty}^{+\infty} dp\, W(x\cos\phi - p\sin\phi,\, x\sin\phi + p\cos\phi). \tag{23}$$

In Figs. 2–4 we plot the marginal distributions $P(x) = P(x,0)$ and $P(y) = P(x,\pi/2)$. The squeezing properties of the quadrature distributions and of the Wigner function are clearly seen in the figures. They relate to reduced/increased widths of the distributions and the humps in appropriate phase space directions or phase angles. In Fig. 5 we represent also the result for minimal (with respect to the phase angle ϕ) dispersion of the quadrature amplitude fluctuations $\langle(\Delta X_\phi)^2\rangle_{\min}$, which is obtained using $P(x,\phi)$. The same result is obtainable if the calculations are carried out on the basis of the operator moments (see Ref. [15] for the details applied to the simplified PDAO model). We note that the squeezing properties in the cases of the monostable and bistable behavior of the semiclassical intensity of the signal mode are essentially different. In particular, in the bistable operation regime (which is actually tristable in the phase-space), the squeezing effect is realized in the below-threshold region only, before the formation of the side-humps in the Wigner function. In the monostable regime the squeezing effect is realized in both the below- and above-threshold regimes. It should be pointed out, that we speak of the squeezing effect within the ranges of the exact nonlinear treatment of quantum fluctuations. In this case the squeezing is referred to the dispersion of quadrature fluctuations with respect to all humps. It is clear, that the minimization of that dispersion is achieved at the phase angle for which the locations of the humps become coincident. However, in the general case this minimal dispersion does not demonstrate reduction of fluctuations below the shot-noise level. In contrast, in the linearized treatment of quantum fluctuations the squeezed noise reduction is referred to the fluctuations with respect to one of the humps. Of course, an individual hump may demonstrate squeezed fluctuations at a particular phase angle. However, this angle does not coincide in the general case with the angle which corresponds to the minimal dispersion in the nonlinear quantum theory.

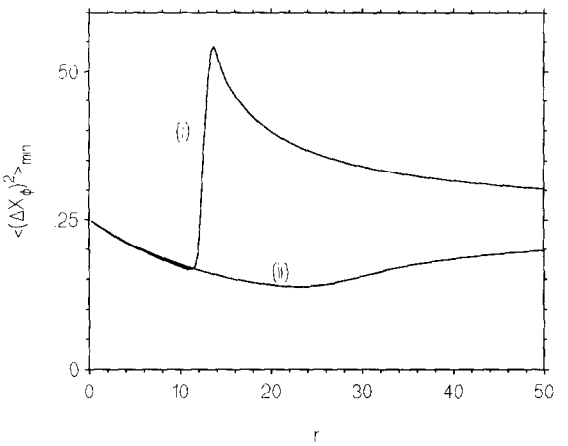

Fig. 5. Minimal dispersion of the quadrature amplitude fluctuations $\langle(\Delta X_\phi)^2\rangle_{\min}$ plotted against r for $\lambda = -20 - 10i$ (curve (i)) and $\lambda = 20 - 10i$ (curve (ii)). The coherent level of fluctuations and the squeezed noise reduction correspond, respectively, to $1/4$ and to $\langle(\Delta X_\phi)^2\rangle < 1/4$.

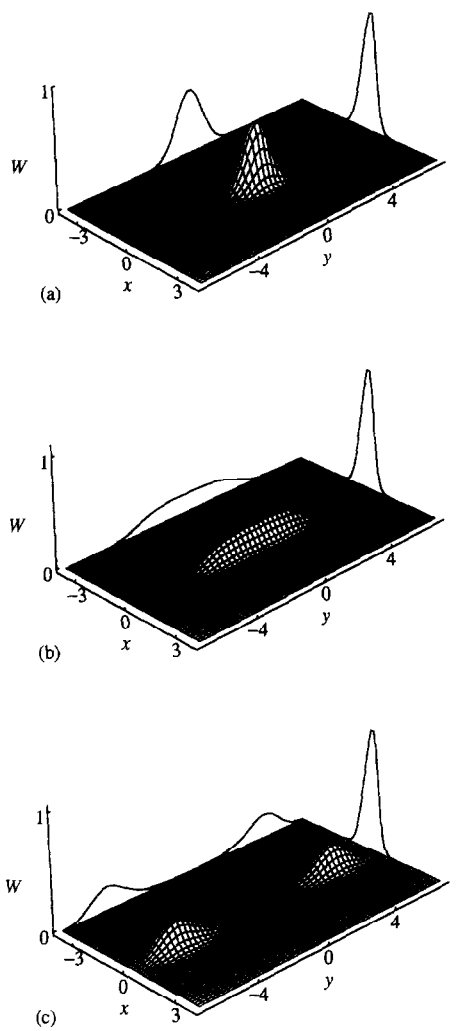

Fig. 4. As in Fig. 3 but for the case of pure PO model with $\lambda = 100$ ($r_{th} = 100$) and $\theta = \pi/4$: (a) $r = 56.25$ (below-threshold regime); (b) $r = 100$ (threshold regime); (c) $r = 121$ (above-threshold regime).

We note that, when considering the steady-state squeezing or other results of the linearized and nonlinear theories with respect to a particular experimental situation, one needs to take into account the corresponding characteristic times of approaching this steady-state regime. The related problem is the characteristic switching times associated with the transition from one steady state to another due to quantum fluctuations. Although, the evaluation of these times for our nonlinear system is beyond the framework of the present paper, the qualitative aspect of the problem is of general character and is well studied for other optically bistable systems (see, e.g., Refs. [17,18]). Actually, the results of the linearized theory correspond to the properties of one of the steady states and to time scales smaller than the characteristic switching times, while the switching times must be exceeded in order to approach the steady state from the strictly statistical viewpoint and to observe the predictions of the nonlinear theory.

6. Oscillatory behavior of the Wigner function in the strong quantum noise limit

The examples of the Wigner function represented in Figs. 2–4 have been given for the case of weak quantum noise strength $|\nu|/|\bar{\gamma}| \ll 1$ ($|\lambda| \gg 1$). In this case the Wigner function does not demonstrate oscillatory behavior or interference fringes, which are known to be indicatives of quantum superposition states (see Ref. [3], and references therein). The oscillatory properties of our Wigner function become revealed in the limit of strong quantum noise. In order to illustrate these properties we consider for simplicity the case $\lambda = 1$ with $r = \mu/\nu$ being real. In this case the Wigner function (13) turns out to be expressed in terms of elementary functions, yielding

$$W_s(x,y) = N\frac{e^{-2y^2}}{x^2+y^2}\left[e^{-2(x-r)^2} + e^{-2(x+r)^2} - 2e^{-2x^2-2r^2}\cos(4ry)\right]. \quad (24)$$

We see here explicitly the appearance of the oscillating term. In order to distinguish the oscillations from the contributions of the first two terms in (24) one needs to consider large r values. In this case, however, the oscillating term becomes extremely small compared with the first two terms. We note also that in the case of $\lambda \sim 1$ the system is still dissipative and hence the quantum coherence properties cannot reveal themselves purely.

In the extreme quantum regime with $\lambda \to 0$, corresponding to vanishing dissipation or very strong coupling, one can obtain from Eq. (13) the following result:

$$W_s(x,y) = Ne^{-2y^2}\left[e^{-2(x-r)^2} + e^{-2(x+r)^2} + 2e^{-2x^2-2r^2}\cos(4ry)\right]. \quad (25)$$

By comparing this result with the Wigner function for the pure superposition of two coherent states $|r\rangle + |-r\rangle$

$$W(x,y) = Ne^{-2y^2}\left[e^{-2(x-r)^2} + e^{-2(x+r)^2} + 2e^{-2x^2}\cos(4ry)\right], \quad (26)$$

we see that the oscillating term in Eq. (25) contains an additional exponential multiplier $\exp(-2r^2)$. This exponent becomes close to unity in the limit $r \ll 1$, and the result (25) approaches in this limit the Wigner function (26) for the superposition of two coherent states. An important difference, however, is that our Wigner function is always positive, while Eq. (26) assumes negative values for arbitrarily small but finite r values. Hence, even in the limit $r \ll 1$ the state of the signal mode cannot be thought of as being in a pure superposition of two coherent states [19], as it has been mentioned in Ref. [12] for the case of pure PO model. This conclusion is in agreement with that of Ref. [14], where a confirming analysis of the corresponding quadrature probabilities has also been carried out. In contrast, the results of the present paper for the generalized PO model allow to provide similar analysis using explicit analytical expressions. Indeed, by using Eq. (23) one can obtain the following simple results for the $P(x)$ and $P(y)$ quadrature probability distributions, corresponding to the Wigner function (25):

$$P_s(x) \propto e^{-2(x-r)^2} + e^{-2(x+r)^2} + 2e^{-2x^2-4r^2}, \quad (27)$$

$$P_s(y) \propto e^{-2y^2}\left[1 + e^{-2r^2}\cos(4ry)\right]. \quad (28)$$

Similarly to the case of the Wigner function (25), our $P_s(x)$ and $P_s(y)$ functions contain an additional $\exp(-2r^2)$ multiplier in the last terms, as compared with the corresponding expressions for the pure superposition state. This multiplier is of crucial importance, when expecting to observe indicatives of quantum superposition – oscillatory behavior or interference fringes. Actually, it masks the cosine oscillations in $P_s(y)$ and the resulting shape of the $P_s(y)$-function does not contain interference minima and maxima.

Acknowledgements

One of us (G.Yu.K.) thanks the Abteilung für Quantenphysik, Universität Ulm for hospitality supported by a DAAD grant. The stimulating discussions with Prof. W.P. Schleich are greatly acknowledged too.

References

[1] C.W. Gardiner, Quantum Noise (Springer, Berlin, 1991).
[2] D.F. Walls and G.J. Milburn, Quantum Optics (Springer, Berlin, 1994).

[3] V. Buzek and P.L. Knight, in: Progress in Optics, Vol. XXXIV, ed. E. Wolf (North Holland, Amsterdam, 1995).
[4] K. Vogel and H. Risken, Phys. Rev. A 40 (1989) 2847.
[5] D.T. Smithey, M. Beck, M.O. Raymer and Faridani, Phys. Rev. Lett. 70 (1993) 1244.
[6] G. Breitenbach, T. Muller, S.F. Pereira, J.-Ph. Poizat, S. Schiller and J. Mlynek, J. Opt. Soc. Am. B 12 (1995) 2304.
[7] P.D. Drummond, K.J. McNeil and D.F. Walls, (a) Optica Acta 27 (1980) 321; (b) 28 (1981) 211.
[8] E. Giacobino, C. Fabre, A. Heidmann, S. Reynaud and L. Lugiato, in: Quantum Optics V, eds. J.D. Harvey and D.F. Walls (Springer, Berlin, 1989).
[9] L. Lugiato, C. Oldano, C. Fabre, E. Giacobino and R. Horowicz, Nuovo Cimento 10 (1988) 959.
[10] Special issue on squeezed states of the electromagnetic field, J. Opt. Soc. Am. B 4, No. 10 (1987).
[11] M.J. Collett and D.F. Walls, Phys. Rev. A 32 (1985) 2887.
[12] M. Wolinsky and H.J. Carmichael, Phys. Rev. Lett. 60 (1988) 1836.
[13] P. Kinsler and P.D. Drummond, Phys. Rev. A 43 (1991) 6194.
[14] M.D. Reid and B. Yurke, Phys. Rev. A 46 (1992) 4131.
[15] G.Yu. Kryuchkyan and K.V. Kheruntsyan, Optics Comm. 127 (1996) 230.
[16] D.A. Kuznetsov, Special Functions (Vysshaya Shkola, Moskva, 1965) [in Russian].
[17] L.A. Lugiato, in: Progress in Optics, Vol. XXI, ed. E. Wolf (North-Holland, Amsterdam, 1984).
[18] P.D. Drummond and P. Kinsler, Phys. Rev. A 40 (1989) 4813; P. Kinsler and P.D. Drummond, Phys. Rev. Lett. 64 (1990) 236.
[19] It should be noted, however, that superpositions may be present in the transient regime of the parametric oscillation [H.J. Carmichael (unpublished)].